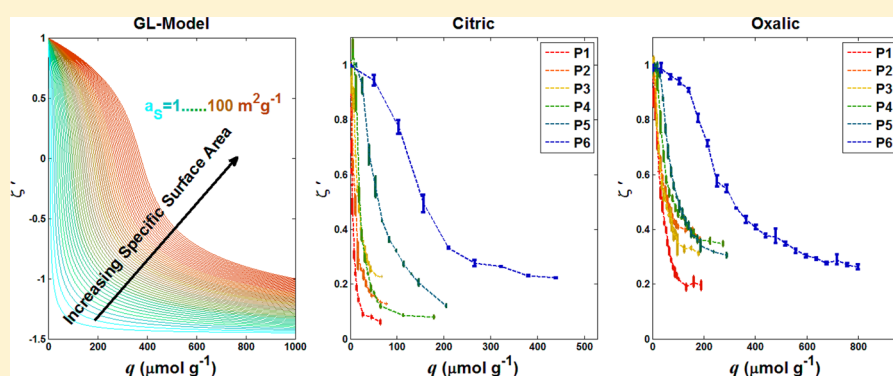


## Scalable Surface Area Characterization by Electrokinetic Analysis of Complex Anion Adsorption

Dorian A. H. Hanaor,\*<sup>†</sup> Maliheh Ghadiri,<sup>‡</sup> Wojciech Chrzanowski,<sup>‡</sup> and Yixiang Gan<sup>†</sup>

<sup>†</sup>School of Civil Engineering and <sup>‡</sup>Faculty of Pharmacy, University of Sydney, Sydney, NSW 2006, Australia

Supporting Information



**ABSTRACT:** By means of the in situ electrokinetic assessment of aqueous particles in conjunction with the addition of anionic adsorbates, we develop and examine a new approach to the scalable characterization of the specific accessible surface area of particles in water. For alumina powders of differing morphology in mildly acidic aqueous suspensions, the effective surface charge was modified by carboxylate anion adsorption through the incremental addition of oxalic and citric acids. The observed zeta potential variation as a function of the proportional reagent additive was found to exhibit inverse hyperbolic sine-type behavior predicted to arise from monolayer adsorption following the Grahame–Langmuir model. Through parameter optimization by inverse problem solving, the zeta potential shift with relative adsorbate addition revealed a nearly linear correlation of a defined surface-area-dependent parameter with the conventionally measured surface area values of the powders, demonstrating that the proposed analytical framework is applicable for the in situ surface area characterization of aqueous particulate matter. The investigated methods have advantages over some conventional surface analysis techniques owing to their direct applicability in aqueous environments at ambient temperature and the ability to modify analysis scales by variation of the adsorption cross section.

### 1. INTRODUCTION

The ability to characterize particle interface structures meaningfully in aqueous media is of importance in a range of high-value industrial processes and applications including catalysis,<sup>1</sup> pharmaceuticals,<sup>2</sup> and water treatment<sup>3</sup> and across the broader field of chemical engineering.

In particulate material, as for natural surfaces in general, a unique value for the specific surface area in terms of area per unit mass cannot be categorically defined. Similarly to the well-known coastline paradox, this results from the scale variance of surface structures.<sup>4,5</sup> Thus, over the past few decades with respect to the assessment of surface-driven material functionality, we commonly speak of the gas-accessible surface area that is most frequently measured by N<sub>2</sub> adsorption in conjunction with BET or Langmuir-type isotherm interpretation for multilayer or monolayer gas adsorption.<sup>6–9</sup> Although improved sensitivity and accuracy are achievable through the adsorption of heavier gases (krypton and argon), such methods nonetheless suffer from known limitations with respect to the measurement scale and conditions.<sup>10,11</sup>

Conventional methods, such as BET, have a clear advantage in facilitating standardized comparative analyses using purposefully built commercially available analytical apparatus. However, there are known drawbacks to the use of such tools. Specifically, gas adsorption methods are limited with respect to (i) the measurement scale (N<sub>2</sub>/O<sub>2</sub>/Kr/Ar exhibit molecular adsorption cross sections in the range of 0.14–0.23 nm<sup>2</sup>);<sup>12</sup> (ii) the measurement temperature (BET analysis is most commonly undertaken at cryogenic temperatures, e.g., 77 K for N<sub>2</sub>); and (iii) the measurement environment (such methods are generally applied to dry powder). The aforementioned scale variance of surface structures means that the assessment of surface area at a constant measurement resolution is problematic. Furthermore, in many applications including catalysis and environmental remediation and in chemical engineering in general, particulate materials are

**Received:** May 12, 2014

**Revised:** October 30, 2014

**Published:** November 27, 2014

applied in an aqueous environment at ambient or high temperatures, thus motivating the adoption of surface area characterization tools that can be applied under analogous conditions with the aim of conducting target-application-relevant interface characterization.

Among alternative adsorption-based surface area analysis methods put forward over recent decades, aqueous- and organic-suspension-based methods feature prominently. Typically the analysis of specific surface area by adsorption in liquid media involves the selection of a material- and application-appropriate adsorbate compound, or “molecular probe”, and the intermittent analysis of an indicative parameter to characterize the presence of residual free adsorbate in interparticle fluid.<sup>13</sup> This is typically achieved *ex situ* using a calorimetric, spectroscopic, titration-based, or visual inspection of interparticle fluids.<sup>14–17</sup> This type of surface characterization is encumbered by the need for parallel analyses and the limitation to systems involving complete or nearly complete adsorption.

The importance of the hierarchical or fractal nature of particle interfaces with surrounding media has resulted in an increasingly wide range of adsorption-based studies addressing the description and measurement of surface area scale variance in particulate materials. Such research efforts were pioneered by studies by Avnir et al. in a series of publications in the 1980s and 1990s.<sup>5,18–22</sup> Conventional nitrogen adsorption isotherms can be interpreted to yield information regarding surface fractality using the Frenkel–Halsey–Hill theory.<sup>20,23</sup> This method has limitations, and its application to systems of unknown surface area is problematic. Further methods to probe the scale variance of small aqueous particles, exhibiting high refractive indices, include laser light scattering interpreted using Rayleigh–Gans–Debye theory.<sup>23,24</sup> More recently, electrochemical approaches to characterizing the roughness and fractal surface structures in electrodes have been reported using cyclic voltammetry, double-layer capacitance analysis, and diffusion-limited current measurements.<sup>25–27</sup> Although not utilized to gauge the accessible surface area, these studies highlight the applicability of using multi-ionic interactions for scalable surface analyses.

Although the formation of multilayers of polyelectrolytes has been reported,<sup>28</sup> the adsorption of complex ions, i.e., molecular ionic species, at aqueous particle surfaces is best described by Langmuir isotherms (type I), which are appropriate because of the electrostatically limited quasi-monolayer-type adsorption exhibited.<sup>29,30</sup> Saturation is approached with increasing adsorbate surface density as the result of the electrostatic repulsion of charged species, limiting further surface ligation.

The electrokinetic behavior exhibited by suspended inorganic particles is known to vary with the adsorption of surfactant molecules to particle surfaces. Recent studies reported the variation of the zeta potential (the electric potential at the shear surface between a particle and its suspending media) with the adsorption of carboxylate anions to surfaces of TiO<sub>2</sub> and ZrO<sub>2</sub>.<sup>31,32</sup> These studies found that the double-layer behavior observed in suspensions was governed by parameters of adsorbate size and particle surface area.

In the present work, we investigate the merit of electrokinetic analyses for the direct assessment of the adsorbate-accessible surface area of aqueous particles in a recirculating suspension. By introducing a new methodology to interpret adsorption isotherms through indicative zeta potential variation, we gauge

the appropriateness of electrokinetic analysis in the analysis of surface structure and particle–reagent interactions.

## 2. METHODOLOGY

Solute ionic adsorbates ligating to particle surfaces in suspension form a quasi-monolayer, the density of which exhibits an electrostatic limit toward steady-state conditions, governed by the size and charge of adsorbates. Consequently, this process can be described by a Langmuir-type adsorption isotherm relating the fractional surface coverage to the adsorbate concentration.<sup>30,33</sup> Fractional surface coverage  $\theta_f \in [0, 1]$  is defined as the ratio of the areal density of surface adsorbed molecules  $N_s$  to the total number of effective surface sites per unit area  $N_{tot}$ . For adsorption from solution to particles with a given total surface area, this is expressed following the Langmuir form as

$$\theta_f = \frac{N_s}{N_{tot}} = \frac{\kappa C}{1 + \kappa C} \quad (1a)$$

Here,  $C$  corresponds to the volumetric concentration of adsorbate in the system, and coefficient  $\kappa$  corresponds to the ratio of adsorption/desorption for a given adsorbate/adsorbent pair such that

$$\kappa = \frac{[AS]}{[A][S]} \quad (1b)$$

where  $[A]$  is the concentration of adsorbate in solution and  $[AS]$  and  $[S]$  represent the surface densities of occupied and unoccupied sites on the adsorbent particles, respectively.  $[A]$  is inversely proportional to the system volume, and  $[S]$  is proportional to the total number of effective surface sites, and thus in monolayer chemisorption for a constant adsorbent mass ( $m_a$ ), coefficient  $\kappa$  is proportional to system volume  $V$  and inversely proportional to the available adsorbent surface area  $A_s$ , which in turn is the product of the specific surface area ( $a_s$ ) and  $m_a$ . An expression to account for specific surface area scaling can be written as

$$\kappa = \kappa' V A_s^{-1}, \theta_f = \frac{\kappa' C V a_s^{-1} m_a^{-1}}{1 + \kappa' C V a_s^{-1} m_a^{-1}} = \left( \frac{\kappa'^{-1} a_s}{q} + 1 \right)^{-1} \quad (2)$$

where  $q = CV/m_a$  corresponds to the quantity of adsorbate per gram of adsorbent (in mol/g).

We can define a surface-area-dependent adsorption coefficient  $K$  [mol/g]:

$$K \propto a_s \text{ such that } K = \kappa'^{-1} a_s \quad (3a)$$

Thus, the expression given in eq 2 simplifies to the expression

$$\theta_f = \frac{1}{K q^{-1} + 1} \quad (3b)$$

The adsorption of complex ions is associated with an increase in surface charge density  $\sigma$  with relation to the charge density of particle surfaces in the absence of adsorbate,  $\sigma_0$ . The density of surface charge in turn governs the electrokinetic parameters.<sup>34</sup>

On the basis of the Gouy–Chapman theory, following the Grahame equation form, the Stern potential  $\psi_\delta$  (in the plane of adsorbed species) and zeta potential  $\zeta$  are generally related to the apparent surface charge,  $\sigma$ , of a suspended particle through an inverse hyperbolic sine relationship of the type given in eq 4.

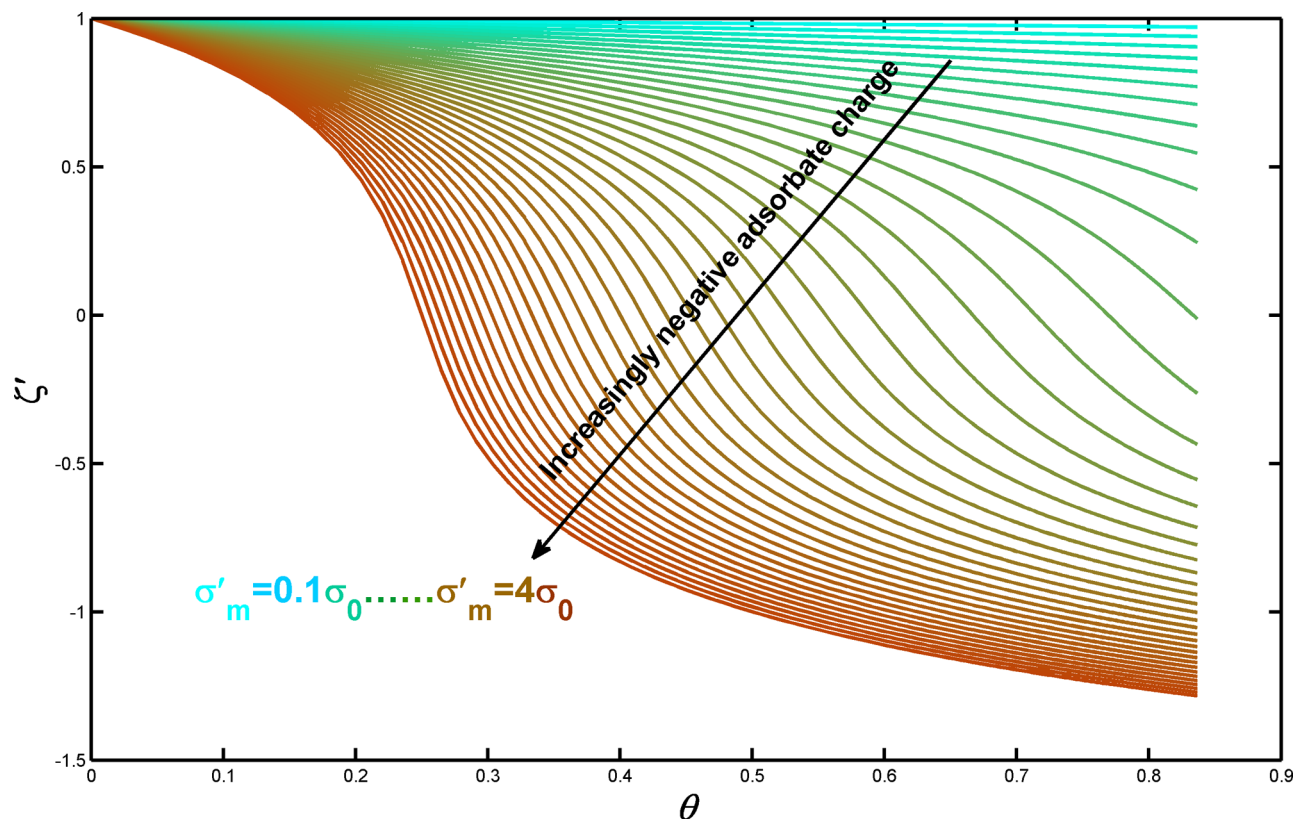


**Figure 1.** Relative zeta potential as a function of the fractional surface coverage for anionic adsorption for a range of different adsorbate anion charge values following eq 5.

$$\zeta = M_1 \operatorname{arcsinh}(M_2 \sigma) \quad (4)$$

Parameter  $\sigma$  may refer to the true surface charge of the solid phase or of the observed Stern-layer charge; accordingly,  $M_1$  is a system constant related to variables of temperature, permittivity, and counterion concentration and speciation, and  $M_2$  is a constant dependent on the temperature and shear plane separation.<sup>35–37</sup>

It has been found that the adsorption of complex ions to particle surfaces in an aqueous suspension is manifest in a shift of the zeta potential with the relative adsorbate concentration following a sigmoidal form with electrokinetic parameters tending toward a quasi-steady state as the adsorption capacity is approached.<sup>31</sup> For the adsorption of anionic species to suspended particles exhibiting initially positive zeta potential values, the shift in zeta potential is expected to exhibit the relationship shown in eq 5 as a function of fractional surface coverage  $\theta$ . Parameter  $\sigma'_m$  corresponds to the net shift in the observed double-layer charge (within the sphere defined by the slipping plane) brought about by monolayer adsorption (occupation of all effective sites) at a surface exhibiting an initial charge of  $\sigma_0$  in the absence of adsorption.

$$\zeta = M_1 \operatorname{arcsinh}[M_2(\sigma_0 - \theta\sigma'_m)] \quad (5)$$

As the adsorption of ionic species in aqueous solution is manifested in the formation of a charged quasi-monolayer, the generalized relationship given by the Grahame–Langmuir model describing the dependence of the potential on adsorbate concentration can be written as

$$\zeta = M_1 \operatorname{arcsinh}\left[M_2\left(\sigma_0 - \frac{\sigma'_m}{(1 + Kq^{-1})}\right)\right] \quad (6)$$

For the anionic adsorption to particles exhibiting an initially positive zeta potential, as studied in the present work, the proportional zeta potential ( $\zeta'$ , taken relative to the initial value of  $\zeta_{(\theta=0)}$ ) exhibits the trend shown in Figure 1 as a function of surface coverage  $\theta$ . Here plots are shown for increasing (negative) adsorbate charge.

In similarity to fractional surface coverage, we can define a readily measurable quantity of fractional zeta potential shift  $\beta \in [0, 1]$  such that

$$\beta = \phi \left| \frac{\zeta - \zeta_0}{\zeta_s - \zeta_0} \right| \quad (7)$$

Under given conditions  $\beta$  represents the double-layer modification at conditions of zeta potential  $\zeta$  relative to the surface-saturated state. Here the value of  $\zeta_0$  corresponds to the zeta potential of suspended particles at the given pH level in the absence of adsorbate and  $\zeta_s$  represents the zeta potential exhibited by suspended particles under conditions equivalent to monolayer coverage ( $\zeta_s = \zeta_{(\theta=1)}$ ).  $\phi$  is a correction factor included to account for the shift in solution parameters, namely, pH and ionic strength, of interparticle fluid (outside the Stern layer) with adsorbate addition. For a system of low solids loading where the ionic strength and pH are assumed to remain sufficiently stable so as not to impart significant  $\zeta$  manipulation, we accept a value of  $\phi = 1$  (and hence  $\beta_{(\theta=1)} = 1$ ).

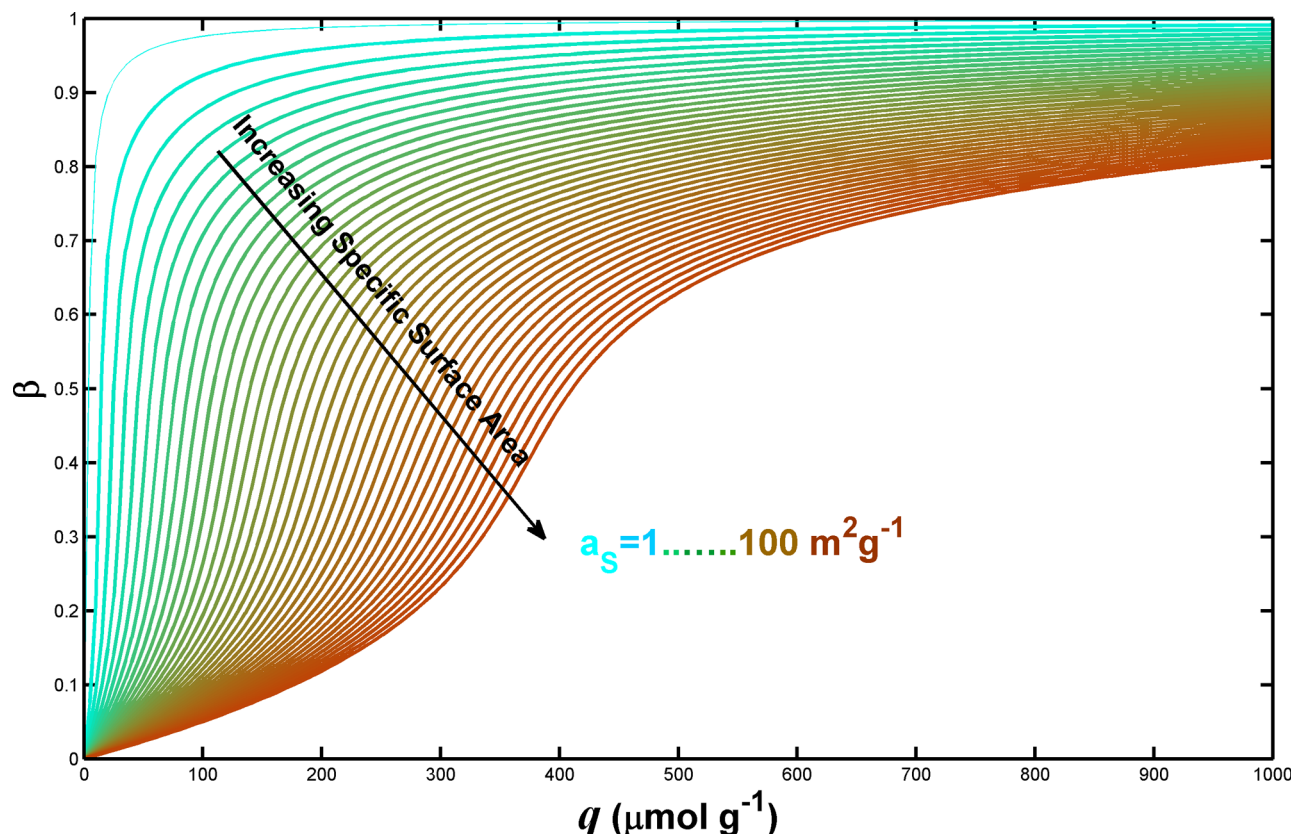


**Figure 2.** Fractional zeta potential shift  $\beta \in [0, 1]$  as a function of additive concentration for a given system volume.

$$\beta = \left| \frac{\operatorname{arcsinh} \left[ M_2 \left( \sigma_0 - \frac{\sigma'_m}{(1 + Kq^{-1})} \right) \right] - \operatorname{arcsinh} [M_2 \sigma_0]}{\operatorname{arcsinh} [M_2 (\sigma_0 - \sigma'_m)] - \operatorname{arcsinh} [M_2 \sigma_0]} \right| \quad (8)$$

Consequently,  $\beta$  is expected to vary following the plot shown in Figure 2. It can be seen that increasing specific surface area, linearly correlated to  $K$ , is manifested in a shift of the sigmoidal relationship.

By zeta potential analysis in conjunction with adsorbate addition, parameter  $\beta$  and its variation can be measured experimentally *in situ* in suspensions or slurries containing particles of unknown surface structure to gauge the accessible surface area per unit mass at tunable scales.

### 3. EXPERIMENTAL PROCEDURES

To evaluate the electrokinetic-based surface characterization of particles in aqueous suspension, calcined and ground high-purity alumina powders ( $\text{Al}_2\text{O}_3$ , Baikowski, >99.9% purity) of varying particle size and specific surface area were chosen as characteristic adsorbent materials. Powder characteristics are summarized in Table 1. The morphology of the powders was assessed by scanning electron microscopy analysis at 5 kV acceleration by means of a Zeiss-Ultra SEM. Zeta potential measurements were carried out using a Malvern Nano ZS analyzer with an automated peristaltic additive dispensing system with suspension recirculation. This apparatus utilizes phase analysis light scattering (PALS) to assess the electrophoretic mobility of particles and thus facilitate the measurement of the zeta potential *in situ* (in the recirculating suspension). Samples were suspended in deionized water to give 10 mL suspensions with a solids loading of 0.1 wt %. To impart positive initial zeta potential values and adequate deflocculation, suspensions were adjusted to pH 4 with the dropwise

**Table 1. Characteristics of Alumina Powders Used in the Present Work**

sample designation	supplier designation	milling method	$\text{Al}_2\text{O}_3$ phases	BET surface area ( $\text{m}^2 \text{g}^{-1}$ )	agglomerate size (nm)
P1	CR1	jet milled	$\alpha$	3	1100
P2	CR6	jet milled	$\alpha$	6	600
P3	SMA6	ball milled	$\alpha$	7	300
P4	CR15	jet milled	90% $\alpha$ , 10% $\gamma$	15	400
P5	CR30F	jet milled	80% $\alpha$ , 20% $\gamma$	26	400
P6	CR12S	jet milled	$\gamma$	105	300

addition of dilute HCl. Citric and oxalic acids (99%, Univar) were used as anionic adsorbates, incrementally added in the form of dilute aqueous solutions to stirring alumina suspensions by means of automated dispensing. For each additive increment, three EK measurements were made with 1 min intervals separating the measurements.

### 4. RESULTS AND DISCUSSION

SEM micrographs of the  $\text{Al}_2\text{O}_3$  powders used are shown in Figure 3. A typical hierarchical microstructure is observed with hard agglomerates consisting of finer primary particles, with the size of primary particles and agglomerate fractality resulting in an increasing specific surface area from P1 to P6.

In similarity to previous observations from  $\text{ZrO}_2$  and  $\text{TiO}_2$  suspensions,<sup>31,32</sup> the addition of dilute citric and oxalic acids to pH 4 alumina suspensions brings about a measurable shift in

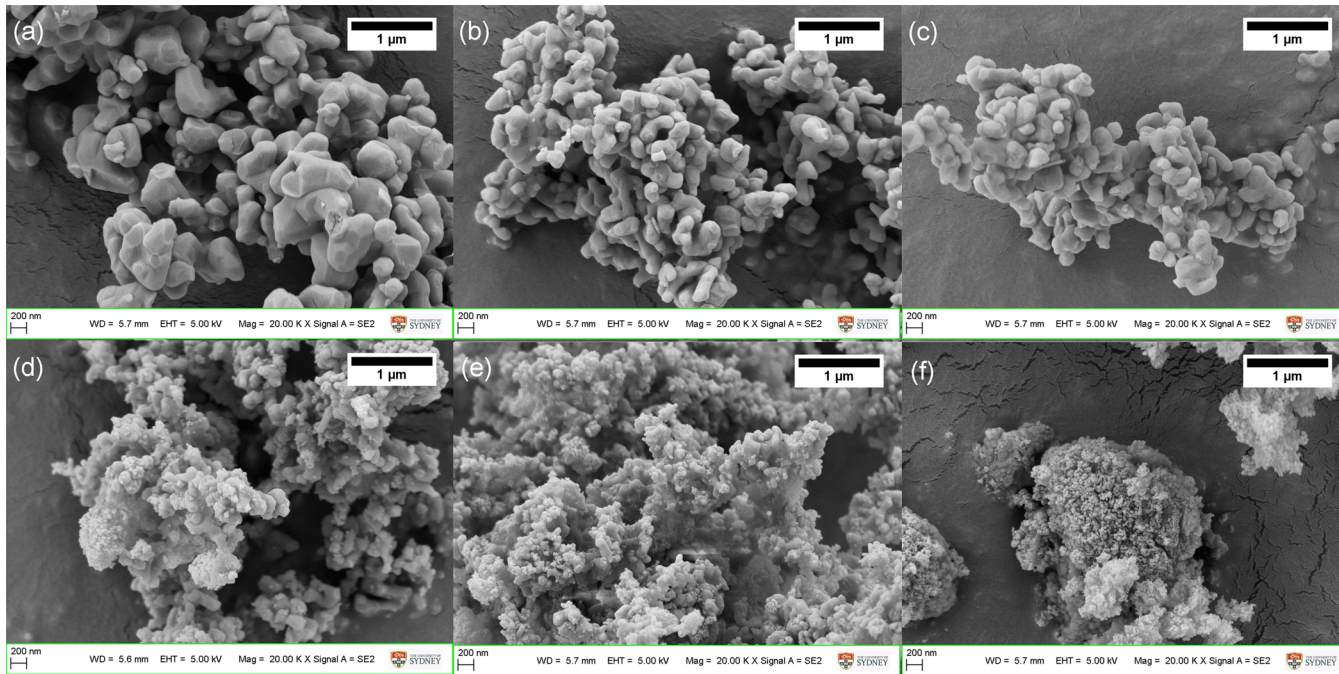


Figure 3. SEM micrographs of  $\text{Al}_2\text{O}_3$  powders used (a–f) corresponding to P1–P6 in Table 1

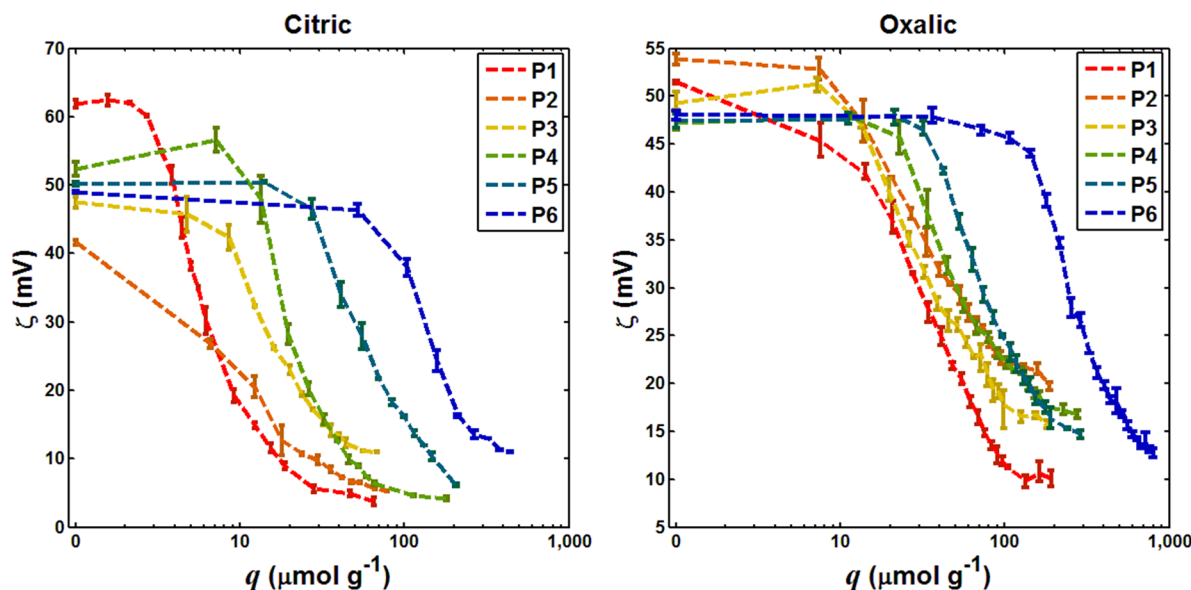
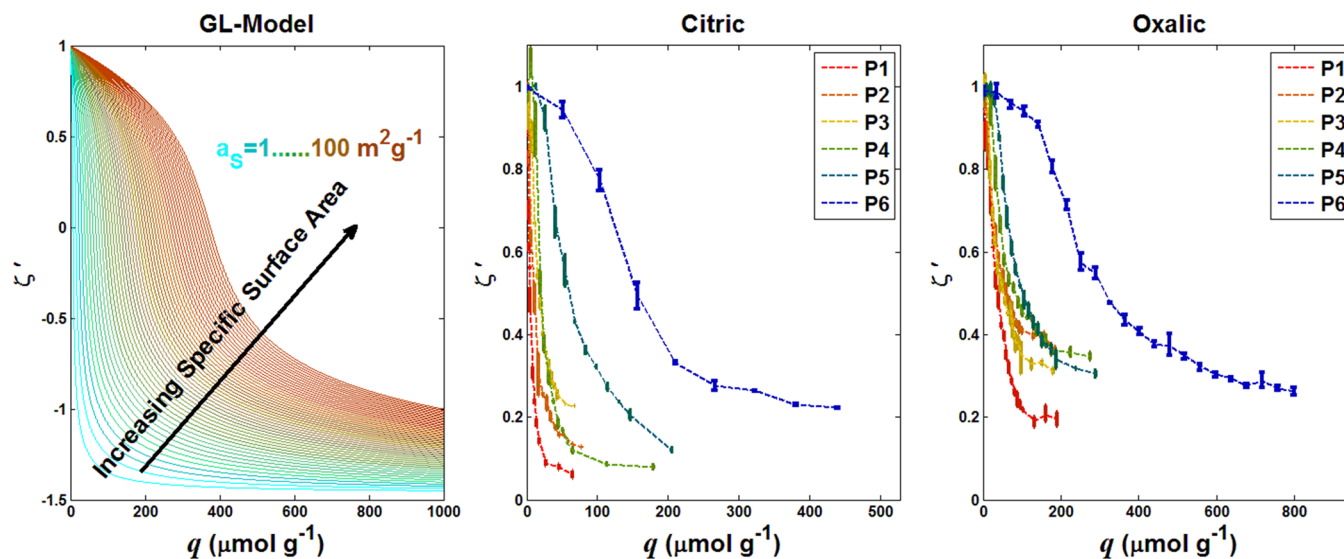


Figure 4. Variation of the zeta potential with additive ratio for powders P1–P6 with citric acid and oxalic acid adsorbates. Vertical bars show the data range at each measurement point.

the electrokinetic properties of suspended particles through the surface adsorption of carboxylate anions. This is shown in Figure 4, where the zeta potential is plotted against the relative adsorbate addition (in proportion to the mass of particles). Here dashed lines show mean values and vertical bars show the data spread. The zeta potential was found to vary from an initial value of  $\sim 45$ – $60$  mV in the HCl-adjusted pH 4 suspension to a final value in the range of 0– $10$  mV subsequent to significant carboxylate addition. From repeated measurement at various concentrations, it was established that for the studied systems the observable change in surface charge resulting from carboxylate adsorption reaches equilibrium in less than 2 min. For this reason, measurements involved an equilibration time

under stirring before repeated zeta potential analyses were carried out.

It can be seen that curves resulting from the use of oxalic acid are shifted to higher relative concentration values (with respect to solids mass) in comparison to the results from citric acid addition owing to the smaller adsorption cross section of oxalate anions relative to citrate. Although being substrate- and speciation-dependent, these cross sections on oxide materials are reported to vary in the regions of  $\sim 0.6$  and  $\sim 1.4$   $\text{nm}^2$  for oxalate and citrate anions, respectively.<sup>38–41</sup> Similarly, with increasing specific surface area (P1–P6), changes in the electrokinetic behavior are observed at higher additive levels. Figure 5 shows the measured relative shift in zeta potential ( $\zeta'$



**Figure 5.** Relative zeta potential shifts resulting from oxalate and citrate adsorption compared to the Grahame–Langmuir model.

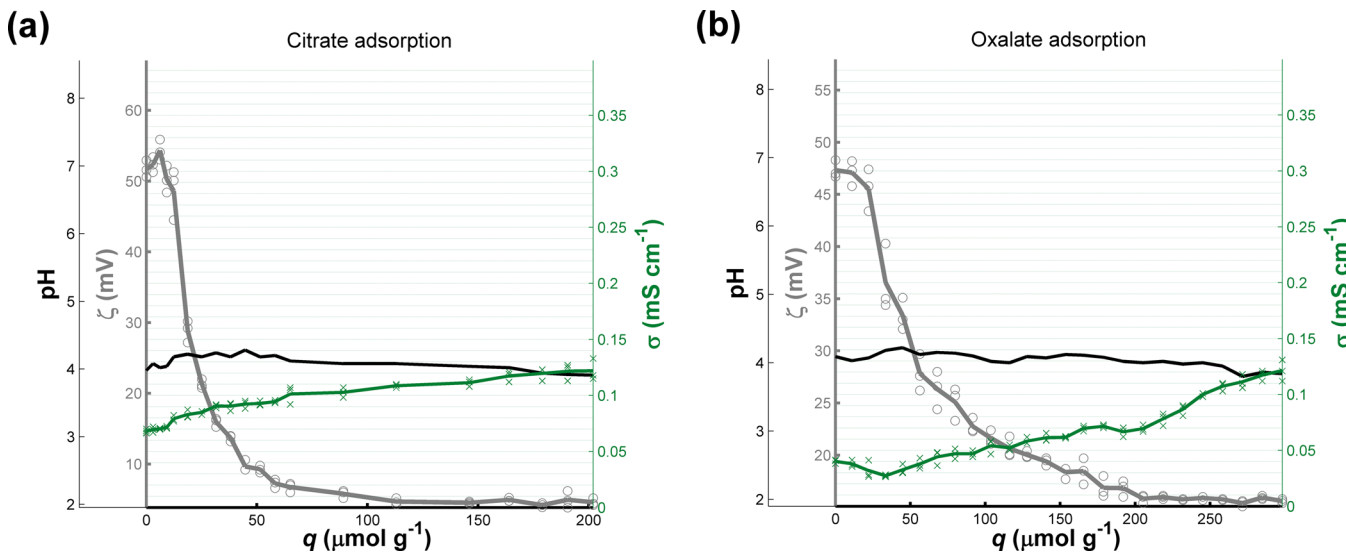


**Figure 6.** Variation of  $\zeta$ , pH, and conductivity in P4 suspensions with (a) citrate and (b) oxalate adsorption.

$= \zeta/\zeta_0$ ) in comparison to that predicted from the Grahame–Langmuir relationship from eq 6.

In addition to facilitating initial deflocculation, the preacidification of suspensions ensured that the observed electrokinetic behavior was mediated by reagent interface interactions rather than by changes to suspension pH or ionic strength. This is further illustrated in Figure 6, showing values for  $\zeta$ , pH, and conductivity during the addition of carboxylic reagents to representative suspensions of P4. The slight decrease in pH would typically be expected to bring about an increase in  $\zeta$  values rather than a decrease, and the moderate increase in suspension conductivity would also not be expected to change the electrokinetic behavior of particles significantly. An initial increase in pH is found in similar systems as the result of the displacement of surface hydroxyls with carboxylate adsorption.<sup>31</sup>

The measurable differences in the indicative electrokinetic behavior seen between substrate powders of different surface area and adsorbates of different size, as shown here, demonstrate the applicability of electrokinetic probing for the

in situ surface area assessments of aqueous particles. Toward this end, parameter fitting by inverse problem solving is carried out in order to evaluate this relationship quantitatively. Although BET measurements are generally limited to the gas-accessible specific surface area relative to N<sub>2</sub> at 77 K (although other gases are utilizable), the present approach gives an additional degree of freedom enabling scale-specific surface characterization at room temperature in aqueous media by using complex ionic adsorbates of varied effective size.

To identify the model parameters, averaged data for the relative shift in zeta potential was interpreted using a parallelized least-squares-type fitting process to determine optimized values for the model parameters in eq 8. Simultaneous multiple parameter optimizations for all particle types were carried out separately for results from both oxalic and citric additives using an unbounded Levenberg–Marquardt algorithm. The tolerance was set as  $1 \times 10^{-14}$ , and convergence was achieved after  $\sim 300$  iterations using centered finite differences for curves for both oxalic and citric adsorbates. In this manner, an optimized  $K$  value for each paring of

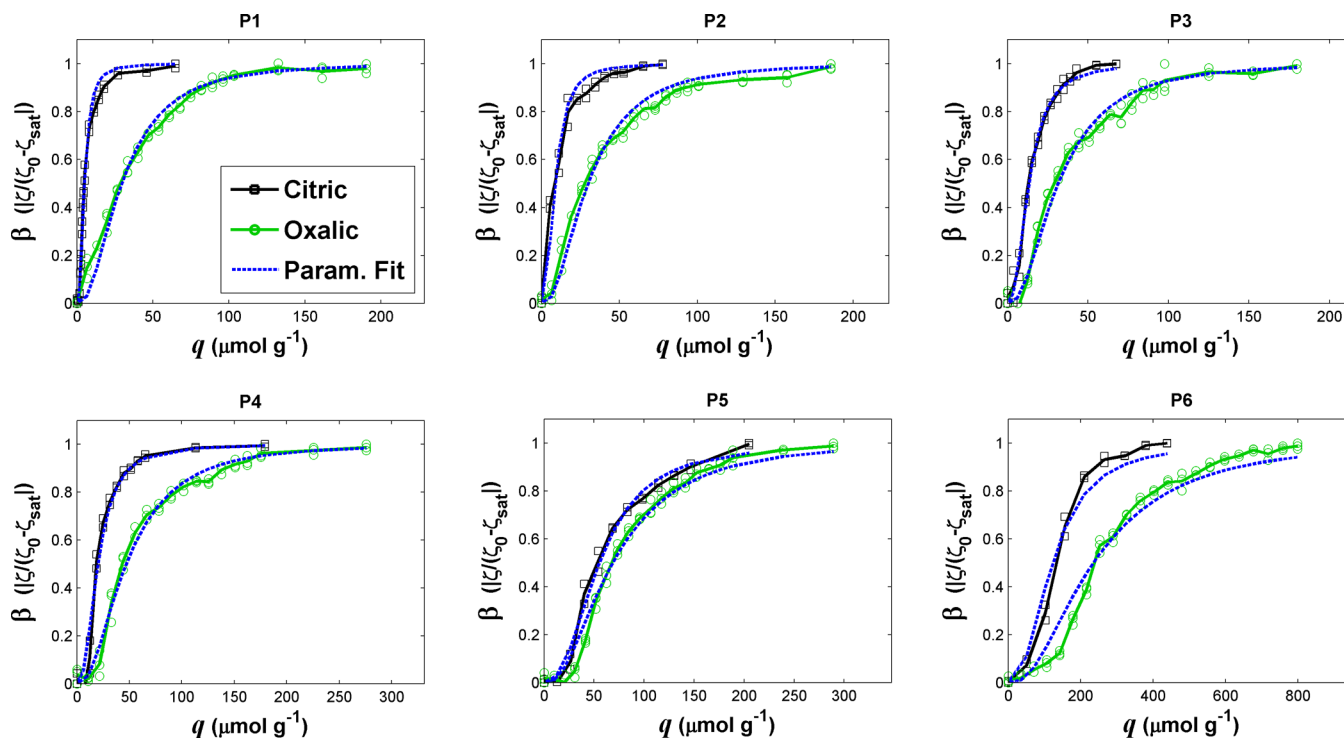


**Figure 7.** Parameter optimization for the fractional  $\zeta$  shift as a function of the proportional additive ratio.

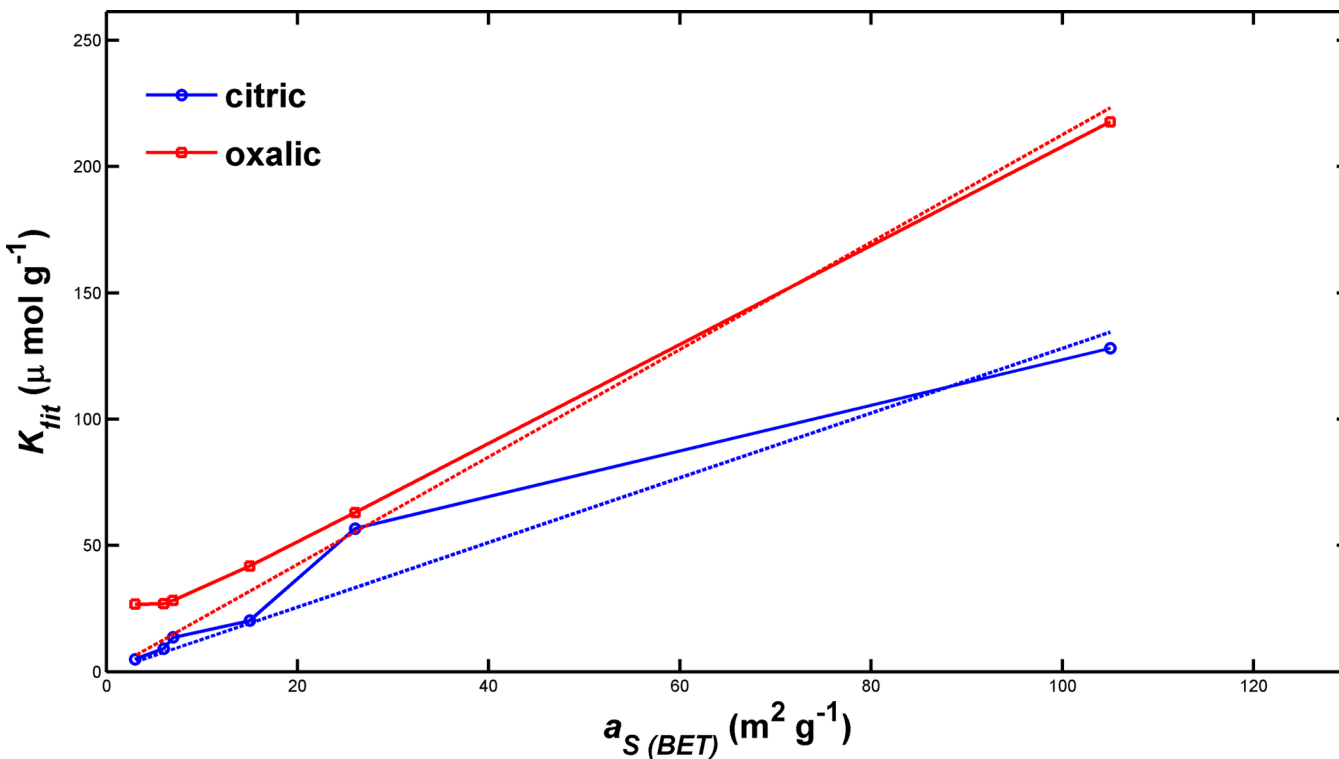


**Figure 8.** Optimized values for surface-area-normalized adsorption coefficient  $K$  plotted against BET measured surface area values.

adsorbent/adsorbate was determined, and optimal values for  $M_2\sigma_0$  and  $M_2\sigma'_m$  were evaluated for both adsorbate reagents optimized to yield the best combined fitting across all six curves in each data set. The results of data fitting for each of the six powders are shown in Figure 7.

The close agreement of the fitted parameters and the experimental data suggests that under the conditions employed,

adsorption behavior followed approximately the monolayer form of the Grahame–Langmuir model. Alternative adsorption models, as may be appropriate for protein/polymer multilayer adsorption or other non-type-I forms<sup>42–44</sup> can facilely be incorporated into the present approach through suitable substitution or adaptation of the Langmuir isotherm form with a more appropriate model for the evaluation of the  $\theta/C$

relationship in the numerical framework used for parameter fitting.

From the data fitting carried out it was determined that for the adsorption of citrate anions the ratio of net negative charge in the apparent Stern plane charge relative to the initial conditions,  $\sigma'_m/\sigma_0$ , was 2.04, whereas for oxalate adsorption this value was optimized at 1.9. These values are indicative of charge density formed by the monolayer adsorption of these carboxylate anions and are dependent on parameters of ion speciation, adsorption/desorption rates, and maximum surface coverage density.

For a given system, the optimized value for parameter  $K$  ( $K_{\text{fit}}$ ) is expected to exhibit a linear dependence on the scale-specific effective surface area, following eq 3. Although no true single value of the specific surface area can be defined, examining the validity of this model requires comparison with a standardized surface area metrology method. Therefore, to assess further the applicability of the current methods toward surface area analysis, we examine the correlation between  $K$  values and the conventional  $N_2$  adsorption-*isotherm*-determined surface area. As shown in Figure 8, this comparison of  $K_{\text{fit}}$  values against the BET-derived surface area for the six powder types shows a trend supporting the linear correlation of fitted  $K$  values with specific surface area. Deviations from linear behavior are expected to result from a combination of (a) fundamental discrepancies between room-temperature anionic adsorption in aqueous media and gas adsorption at low temperatures and (b) experimental uncertainties in establishing and fitting the curves of electrokinetic variation. It is likely that the first parameter is of greater relevance for powders of higher surface area whereas the latter issue plays an important role for substrate materials of lower specific surface area, which exhibit greater sensitivity in their EK behavior.

$K_{\text{fit}}$  values are found to be approximately 1.6–2.0 times higher in results from incremental oxalic acid addition relative to those obtained using the citric additive, which is consistent with the larger adsorption cross section of the citrate anion as reported for various oxide substrates. It should be noted that as with gas adsorption methods<sup>12</sup> the precise adsorptive cross section in terms of  $\text{nm}^2$  per molecule is contingent also on the substrate material and consequently the density of exchangeable surface groups. For this reason, in contrast to comparative analysis, meaningful quantitative analyses require a system-specific calibration to establish a reference point for a known surface area under the given conditions. Furthermore, the monolayer density is affected by the adsorbate speciation, which in turn is influenced by the pH, meaning that significant pH fluctuations would be detrimental to the accuracy of the analysis. For the conditions utilized here (pH 4), oxalate is expected to exhibit a speciation of 57%  $\text{AH}^-$  and 43%  $\text{A}^{2-}$  whereas citrate is expected to speciate following 76%  $\text{AH}_2^-$ , 13%  $\text{AH}^{2-}$ , and 11%  $\text{AH}_3^-$  (where A represents the fully deprotonated molecule).<sup>31</sup>

The approximate linearity of the  $K_{\text{fit}}/a_{S(\text{BET})}$  relationship is indicative of the applicability of electrokinetic analysis for the quantitative or comparative evaluation of surface area. Correlation coefficients of  $R_{\text{citric}}^2 = 0.946$  and  $R_{\text{oxalic}}^2 = 0.965$  were obtained for this relationship fitted to pass through origin  $K_{\text{fit}} (a_S = 0) = 0$ . Owing to the fundamental discrepancies between BET methods and the adsorption methods explored here, it may be appropriate to examine the correlation of results with surface area obtained by ex situ analysis of adsorption (e.g.,

spectroscopic analysis of supernatant fluids) or by microanalytical methods (AFM, SEM, and TEM).

The slope of  $K/a_s (\kappa'^{-1})$  in units of  $\mu\text{mol m}^{-2}$  is proportional to the density of monolayer adsorption. For the fitted data, the slopes of 2.13 and  $1.28 \mu\text{mol m}^{-2}$  for the adsorption of oxalate and citrate, respectively, are in good agreement with previously reported values for these species.<sup>31,45</sup> Applying oxalic  $\kappa'^{-1}$  values in eq 3a together with the  $K_{\text{fit}}$  values allows the evaluation of  $a_s$  values of 12.5, 12.6, 13.3, 19.6, 29.6, and 102.2  $\text{m}^2 \text{g}^{-1}$ , respectively, for materials P1 to P6, whereas the citrate adsorption thus yields values of 3.9, 7.2, 10.6, 15.8, 44.2, and 100.1  $\text{m}^2 \text{g}^{-1}$  for P1 to P6. It is important to note that these values are provisional because they are calculated on the basis of a linear fitting with relation to BET values. Extracting more definitive or meaningful numerical quantities would require the use of one or more reference samples of well-characterized surface structure.

The computational and experimental methods followed here with respect to the analysis of  $\zeta$  variation as a function of mass-relative reagent addition with parameter fitting to the Grahame–Langmuir form to facilitate surface area assessment can be applied with the use of a range of alternative complex cationic and anionic species potentially including, among others, the use of ammonium salts, phosphates/sulfates, xanthates, or polysorbates. The appropriateness of these surface-interacting reagents is coupled to various substrate and system characteristics and necessitates adaptation on a case-by-case basis. Importantly, electrokinetic parameters, determined here by PALS analysis of electrophoresis, can also be measured using alternative techniques including electroosmosis, the streaming potential, and the streaming current. Such methods may be more appropriate for conducting in situ analyses of surface structure in more condensed particle–fluid systems such as slurries. This approach is relevant to the control and optimization of industrial processes where the ability to assess the surface structure of aqueous particles without lengthy ex situ analysis is of value.

## 5. CONCLUSIONS

We have shown a numerical and experimental framework that can be applied to acquire surface structure information through means of electrokinetic characterization. Specifically, the variation of zeta potential exhibited by adsorbent particles as a function of proportional adsorbate concentration follows the Grahame–Langmuir relationship for the monolayer-type adsorption of complex ionic species in aqueous media. The adsorption of carboxylate ions to alumina particles was used to demonstrate the merit of this behavior for the quantitative and comparative characterization of particle surfaces. A nearly linear relationship between the value found from parameter optimization for the surface-area-normalized adsorption coefficient  $K$  and the conventionally determined surface area indicates that the analysis of zeta potential variation (or other electrokinetic properties) in conjunction with the incremental addition of cationic or anionic adsorbates is applicable to the controllable scale-specific evaluation of accessible surface area. By further employing ionic species of a known and controlled adsorption cross section with respect to the substrate material in question, this approach can be used in the assessment of the scale variance of fractal surface structures in aqueous particulate matter.

Using an automated dispersion-measurement system, the experiments carried out here involved in situ electrokinetic

analysis-based surface characterization. Thus, PALS-based measurements and suspension modification were performed on a single recirculating aqueous system. This approach is advantageous relative to the analysis of the gas-accessible surface using N<sub>2</sub> at 77 K because it allows application-relevant room-temperature analysis for aqueous particle–fluid systems in applications including water treatment, photocatalysis, and industrial processing. Furthermore, such methods offer advantages in terms of rapidity and scalability relative to existing aqueous methods for surface area analysis that typically involve intermittent secondary analysis to assess the levels of adsorption density or the concentration of adsorbates in supernatant fluids.<sup>46</sup>

The broad range of acceptable ionic adsorbate compounds that can be employed to facilitate the measurement of surface area by the assessment, *in situ* or otherwise, of indicative electrokinetic or electrochemical parameters is in contrast to existing methods for surface characterization by adsorption isotherm interpretation that are inflexible with respect to surface-interacting compounds and thus do not readily facilitate application-specific analyses and the assessment of scale variance. Although the precise quantitative evaluation of surface area requires calibration with reference to the specimen of known surface area to facilitate back calculation, the use of *in situ* electrokinetic analyses can readily facilitate the comparative analysis between suspended powders of varying surface structures at tunable scales.

## ■ ASSOCIATED CONTENT

### Supporting Information

Zeta potential vs  $\mu\text{mol m}^{-2}$  for oxalic and citric acid. This material is available free of charge via the Internet at <http://pubs.acs.org>.

## ■ AUTHOR INFORMATION

### Corresponding Author

\*E-mail: dorian.hanaor@sydney.edu.au. Phone: +61-404-188810.

### Notes

The authors declare no competing financial interest.

## ■ REFERENCES

- (1) Leofanti, G.; Padovan, M.; Tozzola, G.; Venturelli, B. Surface area and pore texture of catalysts. *Catal. Today* **1998**, *41*, 207–219.
- (2) Paluch, K. J.; Tajber, L.; Corrigan, O. I.; Healy, A. M. Impact of Alternative Solid State Forms and Specific Surface Area of High-Dose, Hydrophilic Active Pharmaceutical Ingredients on Tabletability. *Mol. Pharmaceutics* **2013**, *10*, 3628–3639.
- (3) Sun, D. D.; Wu, Y.; Gao, P. Effects of TiO<sub>2</sub> nanostructure and operating parameters on optimized water disinfection processes: A comparative study. *Chem. Eng. J.* **2014**, *249*, 160–166.
- (4) Mandelbrot, B. B. *The Fractal Geometry of Nature*; W. H. Freeman: New York, 1983.
- (5) Avnir, D.; Farin, D.; Pfeifer, P. Chemistry in noninteger dimensions between two and three. II. Fractal surfaces of adsorbents. *J. Chem. Phys.* **1983**, *79*, 3566–3571.
- (6) Langmuir, I. Vapor pressures, evaporation, condensation and adsorption. *J. Am. Chem. Soc.* **1932**, *54*, 2798–2832.
- (7) Lowell, S.; Shields, J. E. *Powder Surface Area and Porosity*; Chapman and Hall: New York, 1991; Vol. 2.
- (8) Gómez-Serrano, V.; González-García, C.; González-Martin, M. Nitrogen adsorption isotherms on carbonaceous materials. Comparison of BET and Langmuir surface areas. *Powder Technol.* **2001**, *116*, 103–108.
- (9) Barrett, E. P.; Joyner, L. G.; Halenda, P. P. The determination of pore volume and area distributions in porous substances. I. Computations from nitrogen isotherms. *J. Am. Chem. Soc.* **1951**, *73*, 373–380.
- (10) Sing, K. The use of nitrogen adsorption for the characterisation of porous materials. *Colloids Surf., A* **2001**, *187*, 3–9.
- (11) Badalyan, A.; Pendleton, P. Analysis of uncertainties in manometric gas-adsorption measurements. I: Propagation of uncertainties in BET analyses. *Langmuir* **2003**, *19*, 7919–7928.
- (12) Ismail, I. M. Cross-sectional areas of adsorbed nitrogen, argon, krypton, and oxygen on carbons and fumed silicas at liquid nitrogen temperature. *Langmuir* **1992**, *8*, 360–365.
- (13) Fierro, J. G. Chemisorption of probe molecules. *Stud. Surf. Sci. Catal.* **1990**, *57*, B1–B66.
- (14) Kipling, J.; Wilson, R. Adsorption of methylene blue in the determination of surface areas. *J. Appl. Chem.* **1960**, *10*, 109–113.
- (15) Stoeckli, F.; López-Ramón, M. V.; Moreno-Castilla, C. Adsorption of phenolic compounds from aqueous solutions, by activated carbons, described by the Dubinin-Astakhov equation. *Langmuir* **2001**, *17*, 3301–3306.
- (16) Dąbrowski, A. Adsorption—from theory to practice. *Adv. Colloid Interface Sci.* **2001**, *93*, 135–224.
- (17) Wang, S.-L.; Johnston, C. T.; Bish, D. L.; White, J. L.; Hem, S. L. Water-vapor adsorption and surface area measurement of poorly crystalline boehmite. *J. Colloid Interface Sci.* **2003**, *260*, 26–35.
- (18) Avnir, D. Fractal Aspects of Surface Science—An Interim Report, *Material Research Society Symposium Proceedings*; Cambridge University Press: New York, 1986; pp 321–329.
- (19) Avnir, D.; Farin, D.; Pfeifer, P. Molecular fractal surfaces. *Nature* **1984**, *308*, 261–263.
- (20) Avnir, D.; Jaroniec, M. An isotherm equation for adsorption on fractal surfaces of heterogeneous porous materials. *Langmuir* **1989**, *5*, 1431–1433.
- (21) Farin, D.; Avnir, D. The fractal nature of molecule-surface chemical activities and physical interactions in porous materials. *Characterization of Porous Solids*; Elsevier: Amsterdam, 1988; pp 421–432.
- (22) Farin, D.; Avnir, D. Surface fractality of dendrimers. *Angew. Chem., Int. Ed. Engl.* **1991**, *30*, 1379–1380.
- (23) Tang, P.; Chew, N. Y.; Chan, H.-K.; Raper, J. A. Limitation of determination of surface fractal dimension using N<sub>2</sub> adsorption isotherms and modified Frenkel-Halsey-Hill theory. *Langmuir* **2003**, *19*, 2632–2638.
- (24) Block, J. M.; Keer, L. M. Periodic contact problems in plane elasticity. *J. Mech. Mater. Struct.* **2008**, *3*, 1207–1237.
- (25) Go, J.-Y.; Pyun, S.-I. Fractal Approach to Rough Surfaces and Interfaces in Electrochemistry. *Modern Aspects of Electrochemistry*; Springer: New York, 2006; Vol. 39, pp 167–229.
- (26) Go, J.-Y.; Pyun, S.-I.; Hahn, Y.-D. A study on ionic diffusion towards self-affine fractal electrode by cyclic voltammetry and atomic force microscopy. *J. Electroanal. Chem.* **2003**, *549*, 49–59.
- (27) Daikhin, L.; Kornyshev, A.; Urbakh, M. Double layer capacitance on a rough metal surface: surface roughness measured by Debye ruler. *Electrochim. Acta* **1997**, *42*, 2853–2860.
- (28) Hoogeveen, N. G.; Cohen Stuart, M. A.; Fleer, G. J.; Böhmer, M. R. Formation and stability of multilayers of polyelectrolytes. *Langmuir* **1996**, *12*, 3675–3681.
- (29) Faria, P.; Orfao, J.; Pereira, M. Adsorption of anionic and cationic dyes on activated carbons with different surface chemistries. *Water Res.* **2004**, *38*, 2043–2052.
- (30) Connor, P.; McQuillan, A. J. Phosphate adsorption onto TiO<sub>2</sub> from aqueous solutions: an *in situ* internal reflection infrared spectroscopic study. *Langmuir* **1999**, *15*, 2916–2921.
- (31) Hanaor, D.; Michelazzi, M.; Leonelli, C.; Sorrell, C. C. The effects of carboxylic acids on the aqueous dispersion and electrophoretic deposition of ZrO<sub>2</sub>. *J. Eur. Ceram. Soc.* **2012**, *32*, 235–244.
- (32) Hanaor, D.; Michelazzi, M.; Veronesi, P.; Leonelli, C.; Romagnoli, M.; Sorrell, C. Anodic aqueous electrophoretic deposition

of titanium dioxide using carboxylic acids as dispersing agents. *J. Eur. Ceram. Soc.* **2011**, *31*, 1041–1047.

(33) Sposito, G. *The Surface Chemistry of Natural Particles*; Oxford University Press: New York, 2004; Vol. 389.

(34) Haydon, D. A study of the relation between electrokinetic potential and surface charge density. *Proc. R. Soc. London, Ser. A* **1960**, *258*, 319–328.

(35) Butt, H.-J.; Graf, K.; Kappl, M. *Physics and Chemistry of Interfaces*; John Wiley & Sons: New York, 2006.

(36) Ohshima, H.; Nakamura, M.; Kondo, T. Electrophoretic mobility of colloidal particles coated with a layer of adsorbed polymers. *Colloid Polym. Sci.* **1992**, *270*, 873–877.

(37) Yang, K.-L.; Ying, T.-Y.; Yiakoumi, S.; Tsouris, C.; Vittoratos, E. S. Electrosorption of ions from aqueous solutions by carbon aerogel: an electrical double-layer model. *Langmuir* **2001**, *17*, 1961–1969.

(38) Hidber, P.; Graule, T.; Gauckler, L. Carboxylic acids as dispersants for alumina slurries. *Handb. Charact. Technol. Solid-Solution Interface* **1993**, 247–254.

(39) Mesuere, K.; Fish, W. Chromate and oxalate adsorption on goethite. 2. Surface complexation modeling of competitive adsorption. *Environ. Sci. Technol.* **1992**, *26*, 2365–2370.

(40) Hug, S. J.; Sulzberger, B. In situ Fourier transform infrared spectroscopic evidence for the formation of several different surface complexes of oxalate on TiO<sub>2</sub> in the aqueous phase. *Langmuir* **1994**, *10*, 3587–3597.

(41) Curreri, P.; Onoda, G.; Finlayson, B. A comparative appraisal of adsorption of citrate on whewellite seed crystals. *J. Cryst. Growth* **1981**, *53*, 209–214.

(42) Rezwan, K.; Meier, L. P.; Rezwan, M.; Vörös, J.; Textor, M.; Gauckler, L. J. Bovine serum albumin adsorption onto colloidal Al<sub>2</sub>O<sub>3</sub> particles: A new model based on zeta potential and UV-vis measurements. *Langmuir* **2004**, *20*, 10055–10061.

(43) Xu, T.; Fu, R.; Yan, L. A new insight into the adsorption of bovine serum albumin onto porous polyethylene membrane by zeta potential measurements, FTIR analyses, and AFM observations. *J. Colloid Interface Sci.* **2003**, *262*, 342–350.

(44) Suksri, H.; Pongjanyakul, T. Interaction of nicotine with magnesium aluminum silicate at different pHs: characterization of flocculate size, zeta potential and nicotine adsorption behavior. *Colloids Surf., B* **2008**, *65*, 54–60.

(45) Hidber, P. C.; Graule, T. J.; Gauckler, L. J. Citric acid—a dispersant for aqueous alumina suspensions. *J. Am. Ceram. Soc.* **1996**, *79*, 1857–1867.

(46) Montes-Navajas, P.; Asenjo, N. G.; Santamaría, R.; Menendez, R.; Corma, A.; García, H. Surface Area Measurement of Graphene Oxide in Aqueous Solutions. *Langmuir* **2013**, *29*, 13443–13448.